Genetic and Biochemical Characterization of a Novel Alkaline-tolerant Xaa-Pro Dipeptidase from Aspergillus phoenicis

Zixing Dong *, Shuangshuang Yang , Kun Zhang , Cunduo Tang , Yunchao Kan , Lunguang Yao *

Posted Date: 20 October 2023

doi: 10.20944/preprints202310.1370.v1

Keywords: Xaa-Pro dipeptidase; Aspergillus phoenicis; reclassification; heterologous expression; biochemical characterization

Article

Genetic and Biochemical Characterization of a Novel Alkaline-Tolerant Xaa-Pro Dipeptidase from *Aspergillus phoenicis*

Zixing Dong [1,*,†], Shuangshuang Yang [2,†], Kun Zhang [1], Cunduo Tang [1,3], Yunchao Kan [1,3] and Luanguang Yao [1,4,*]

[1] Henan Provincial Engineering Laboratory of Insect Bio-Reactor, College of Life Science and Agricultural Engineering, Nanyang Normal University, Nanyang 473061, China
[2] College of Physical Education, Nanyang Normal University, Nanyang 473061, China
[3] China-UK-NYNU-RRes Joint Laboratory of Insect Biology, Henan Key Laboratory of Insect Biology in Funiu Mountain, Nanyang Normal University, Nanyang 473061, China
[4] Henan Provincial Engineering and Technology Center of Health Products for Livestock and Poultry, Nanyang Normal University, Nanyang 473061, China
* Correspondence: star1987.com@163.com (Z.D.); lunguangyao@163.com (L.Y.); Tel.: +86-0377-63525087 (L.Y)
† These authors contributed equally to this work.

Abstract: Xaa-Pro dipeptidase (XPD, EC 3.4.13.9; also known as prolidase) catalyzes the hydrolysis of iminopeptide bond in the trans Xaa-Pro dipeptides (Xaa represents any amino acid except proline), which makes it find wide applications in food, medical and environmental protection fields. In the present study, a novel Xaa-Pro dipeptidase from *Aspergillus phoenicis* ATCC 14332 (ApXPD) was molecularly and biochemically characterized. Reclassification based on phylogenetic analysis and version 12.5 MEROPS database showed that this enzyme was the only fungal XPD in the unassigned subfamily which shared the highest sequence similarity with *Xanthomonas campestris* prolidase but not with that from the more related fungal species *A. niudulans*. As compared with other prolidases, ApXPD also contained an N-terminal tail (residues 81-89) and an additional region (PAPARLREKL), and used a different arginine residue for dipeptide selectivity. After heterologous expression and partial purification, recombinant ApXPD was highly active and stable over the alkaline range from 8.5 to 10.0, with a maximum activity at pH 9.0 and more than 80% activity retained after 1-h incubation at pHs of 8.5-10.0 (55 °C). It also had an apparent optimum temperature of 55 °C and remained stable at 20–30 °C. Moreover, this enzyme was a cobalt dependent prolidase that only cleaved dipeptides Lys-Pro, Gly-Pro and Ala-Pro rather than other dipeptides, tripeptides and tetrapeptides. All these distinct features make *A. phoenicis* ATCC 14332 XPD unique among currently known prolidases, thus defining a novel Xaa-Pro dipeptidase subfamily.

Keywords: Xaa-Pro dipeptidase; *Aspergillus phoenicis*; reclassification; heterologous expression; biochemical characterization

1. Introduction

Xaa-Pro dipeptidase (XPD, EC 3.4.13.9), also called prolidase, proline dipeptidase, peptidase D (PEPD), imidodipeptidase or organophosphorus anhydrase (OPAA), is the only enzyme catalyzing the hydrolysis of iminopeptide bond in a trans Xaa-Pro dipeptide (Xaa represents any amino acid except proline) and belongs to subfamily M24B within clan MG of metallopeptidases in the version 12.5 MEROPS database (https://www.ebi.ac.uk/merops/) [1]. XPDs are found in all living organisms and have been isolated mainly from mammalian tissues, fungi, archaea and eubacteria [2,3]. Although the physiological roles of prolidases in bacteria and archaea remain unclear, they are thought to act along with other endo- and/or exopeptidases in proline recycling and antitoxin defense [4-6]. In mammals, the physiological roles of XPDs are well established in different patho-physiological conditions. Moreover, human prolidases are involved in collagen turnover, matrix remodeling and protein metabolism [2,3], and they therefore play vital roles in several physiological

 doi:10.20944/preprints202310.1370.v1

processes including inflammation, carcinogenesis, wound healing, angiogenesis and cell proliferation, especially a rare hereditary syndrome called prolidase deficiency [5,7].

Xaa-Pro dipeptidases find extensive use in food, environmental protection and medical fields. Because they can hydrolyze proline-containing peptides responsible for bitter flavor in cheese, these enzymes have been used in dairy industry to lower cheese bitterness, thus enhancing its flavor [8]. Organophosphorus (OP) cholinesterase-inhibiting compounds are constituents of many chemical nerve agents and pesticides. Some XPDs also exhibit OPAA activity and can detoxify these OP compounds by cleaving the P-F and P-O bonds, and this ability makes them serve as biosensors or environmentally friendly decontaminating agents to detect/degrade OP pesticides and chemical warfare nerve agents [9,10]. Currently, several approaches, such as immobilization [11] and protein engineering [12,13], have also been adopted to improve the OPAA activities of several XPDs. Directed evolution of PlOPAA led to a 30-fold increase in paraoxon hydrolysis [12] and 10000-fold increase in methyl-parathion hydrolysis [13], respectively. In addition, human prolidase can be employed as prodrug therapeutic agents and potential biomarkers for prolidase deficiency [14], cancer, diabetes, brain diseases, liver diseases, respiratory diseases, and many other disorders [2,7].

The fungi are always amongst the best enzyme producers. To date, however, only one fungal Xaa-Pro dipeptidase (GenBank accession No. CAC39600.1) has been molecularly and biochemically characterized from *Aspergillus nidulans* [15]. *A. phoenicis* is an interesting thermotolerant fungus which grows well at 42-45°C. Due to its great hydrolytic potential, *A. phoenicis* synthesizes many enzymes with various applications in the biotechnological industry, including carbohydrases, proteases, lipases and chitinases [16,17], as well as several oxidoreductases, such as laccases [16], catalases [18] and glucose dehydrogenases [19]. In July 2018, the release of the genome sequence of *A. phoenicis* ATCC 13157 has opened up opportunities to molecularly and biochemically characterize its proteolytic enzymes for industrial applications and investigate their exact physiological roles. However, only few of these proteases have been biochemically and functionally identified based on latest literature survey.

Examination of the genome sequence of *A. phoenicis* ATCC 13157 has revealed that it encodes at least one putative prolidase. In the present study, a putative Xaa-Pro dipeptidase gene (GenBank accession No. KZ851879.1) was cloned from *A. phoenicis* ATCC 14332 and expressed in *Pichia pastoris*. After partial purification, its biochemical characteristics were systematically investigated. Our results will provide a novel insight into fungal XPDs, and may facilitate further studies on the physiological roles of this prolidase.

2. Materials and Methods

2.1. Chemicals and Reagents

Restriction enzymes, T_4 DNA ligase, Pyrobest™ DNA polymerase, DNA Fragment Purification Kit, Agarose Gel DNA Extraction Kit, and Plasmid Purification Kit were purchased from TaKaRa Bio Inc. (Dalian, P.R. China). High Pure RNA Isolation Kit and Transcriptor High Fidelity cDNA Synthesis Kit were the products of Roche Molecular Biochemicals (QC, Canada). Tryptone and yeast extract were bought from OXOID (Basingstoke, UK). Casein, and prestained protein marker were supplied by Sigma-Aldrich (Shanghai, P.R. China), and Thermo Fisher Scientific (Shanghai, P.R. China), respectively. Dipeptides, tripeptides and tetrapeptides were purchased from Ontores Biotechnologies (Hangzhou, P.R. China). All other chemicals were commercially available in analytical grade.

2.2. Plasmids, Strains and Growth Conditions

Shuttle vector pPIC9K (Invitrogen; Carlsbad, CA, USA) was used for gene cloning and expression. *A. phoenicis* ATCC 14332 bought from ATCC (USA) served as a template for *apxpd* gene cloning. *Escherichia coli* JM109 and *P. pastoris* GS115 (Invitrogen) were employed as the hosts for plasmid amplification and gene expression, respectively. *A. phoenicis* ATCC 14332 and *E. coli* JM109 were respectively grown in PDA medium (20% (w/v) potato, 2% dextrose, 2% agar) containing 1%

Preprints (www.preprints.org) | NOT PEER-REVIEWED | Posted: 20 October 2023 doi:10.20944/preprints202310.1370.v1

(w/v) casein and Luria-Bertani (LB) medium (1% (w/v) tryptone, 0.5% yeast extract, and 1% NaCl). To cultivate *P. pastoris* GS115 and its recombinants, yeast extract peptone dextrose (YPD) medium, minimal dextrose (MD) medium, the buffered minimal glycerol-complex (BMGY) medium, and the buffered minimal methanol-complex (BMMY) medium were prepared according to the manufacturer's protocols.

2.3. Gene Cloning and Sequence Analysis

Total RNA of *A. phoenicis* ATCC 14332 was extracted and reverse transcribed into cDNA by the kits according to manufacturer's instructions. Using the cDNA obtained as a template, *apxpd* gene was amplified by PCR with primers ApXPD1 (5′-GTACTGGACAAACAGACTGAGTCTCTCCC-3′) and ApXPD2 (5′-TGCTCTAGACTATGGGTCCCAAGGCCCATAT-3′; the *Xba*I restriction site is underlined). The PCR products were then cut by *Xba*I, purified with DNA Fragment Purification Kit, and ligated with *Sna*BI/*Avr*II-digested pPIC9K, generating the recombinant plasmid pPIC9K-apxpd. After this plasmid was transformed into *E. coli* JM109, positive clones were selected on LB plates supplemented with 100 μg/mL ampicillin. The correctness of the inserted sequence was subsequently confirmed by *Pst*I-digested restriction pattern and DNA sequencing (Sangon Biotech Co., Ltd., Shanghai, P.R. China).

Based on the deduced full-length amino acid sequence of ApXPD, its phylogenic relationships with other known Xaa-Pro dipeptidases were investigated by an evolutionary tree which was constructed by program MEGA version X using the Neighbor-joining algorithm [20]. Bootstrap resampling with 1000 pseudoreplicates was conducted to assess support for each individual branch. Prolidase family was designated by reference to the peptidase deposited in MEROPS database [1]. The online server SignalP 5.0 (https://services.healthtech.dtu.dk/service.php?SignalP-5.0) was used to predict the signal peptide cleavage sites of these XPDs. Multiple sequence alignment was performed with Clustal X2 and BioEdit 7.0.9 software packages. The three-dimensional structure of ApXPD was constructed by homology modeling using the Swiss-Model server (http://swissmodel.expasy.org), with the crystal structure of Xaa-Pro dipeptidase from *Xanthomonas campestris* pv. *campestris* ATCC 33913 (XcXPD, PDB code: 5fcf) [4] as a template. The fine structure of XPD was then generated and visualized by software Discovery Studio 3.5 (Accelrys, USA).

2.4. Expression of ApXPD in P. pastoris

After the correct recombinant plasmid pPIC9K-apxpd was linearized by *Sac*I, it was electroporated into *P. pastoris* GS115 by a Gene Pulser X-cell II electroporation system (Bio-Rad, USA) under conditions of 1.5 kV, 200 Ω, and 25 μF. His^+ transformants were selected on MD plates containing 0.5, 1.0, 1.5 and 2.0 mg/mL G418 with the replica plating method, and the genomic DNAs of these His^+ transformants were then extracted and analyzed by PCR to confirm gene integration.

A single colony of the His^+ transformants exhibiting resistance to 2.0 mg/mL G418 was inoculated into 25 mL BMGY medium and cultivated at 30°C and 200 rpm, until the optical density at 600 nm (OD_{600}) reached 4-6. The growing cells were then harvested by centrifugation (10,000×g, 4°C; 10 min), resuspended in 25 mL BMMY medium to an OD_{600} of 1.0, and cultured at 30°C and 220 rpm for 120 h. To maintain induction, the cultures were fed with pure methanol to a final concentration of 0.5% (v/v) at 24-h intervals. Induction of GS115-9K cells (*P. pastoris* GS115 integrated with pPIC9K) was performed in parallel as a negative control. The supernatants were collected by centrifugation at 10,000×g and 4°C for 10 min, and used for the analysis of XPD activity. Sodium dodecyl sulfate polyacrylamide gel electrophoresis (SDS-PAGE) was also performed to confirm the expression of ApXPD, using 12% (w/v) polyacrylamide gels (1 mm thickness).

2.5. Enzyme Purification

Unless otherwise stated, all purification procedures are performed at 4°C. The cell-free supernatant was fractionated with solid ammonium sulfate at 30-70% saturation. The pellet collected by centrifugation (10,000×g, 4°C; 20 min) was resuspended in a minimal volume of 20 mM Tris-HCl

 doi:10.20944/preprints202310.1370.v1

buffer (pH 8.0)/1 mM cobalt chloride and dialyzed extensively against the same buffer. The dialyzed sample was then concentrated and desalted using a VivaFlow 50 tangential flow filtration module (Vivascience, Sartorius group) with a polyethersulfone membrane (MWCO, 10 kDa). The resulting sample was used for enzyme assay and SDS-PAGE analysis.

2.6. Enzyme and Protein Assays

The ninhydrin method [21] was slightly modified to determine the amount of proline liberated from the peptide substrates. Briefly, the reaction mixture consisted of 2 mM Lys-Pro or other dipeptides, 20 mM Tris-HCl buffer (pH 8.0) and 1 mM cobalt chloride. After the addition of enzyme solution, the reaction mixture was incubated at 55°C for 10 min. An aliquot (200 μL) was withdrawn and mixed with 500 μL of glacial acetic acid and 500 μL of ninhydrin reagent (3% (w/v) ninhydrin, 60% (v/v) glacial acetic acid and 40% (v/v) phosphoric acid). After boiling for 10 min, the solution was cooled on ice. The resulting chromophore was quantified using 515 nm absorption. All measurements were performed in triplicate. One unit of Xaa-Pro dipeptidase activity is defined as the amount of enzyme liberating 1 μmol proline per minute under assay conditions. Protein concentrations were measured by the Bradford Protein Assay Kit (Beyotime Biotechnology, Nantong, China), using bovine serum albumin as a standard.

2.7. Biochemical Characterization of Recombinant ApXPD

The optimal temperature of the purified ApXPD was determined in reactions using fresh enzyme at various temperatures (20, 30, 35, 40, 45, 50 55, 60, 65 and 70°C). To determine its thermostability, recombinant ApXPD was pre-incubated in 20 mM Tris-HCl buffer (pH 8.0) containing 1 mM cobalt chloride at 20, 30, 40, 50, 60 or 70°C for 1 h, prior to standard enzyme assay. All determinations were carried out in triplicate, and the results were presented as the percentage of the activity measured compared with the maximum activity.

The optimum pH of recombinant ApXPD was examined using the following buffer solutions in place of the Tris-HCl buffer in the method described above: 20 mM sodium citrate buffer (pH 6.0-7.5), 20 mM Tris-HCl buffer (pH 7.5-9.0) and 20 mM glycine-NaOH buffer (pH 9.0-10.5). The pH stability was determined by pre-incubation of the purified enzyme in the abovementioned buffers at its optimum temperature for 1 h, followed by measurement of the residual activity under standard assay conditions.

To investigate the effects of various metal ions on the activity of recombinant ApXPD, they were added as the salts of chloride to the reaction mixtures at a final concentration of 0.1 mM or 1 mM. The procedure used to determine the effect of EDTA was the same as above described. The activity of recombinant ApXPD without any additions was set as 100%.

Relative substrate specificity of the recombinant ApXPD was determined in the presence of 1 mM Co^{2+}, using 2 mM various dipeptides (Lys-Pro, Gly-Pro, Ala-Pro, Pro-Pro, Cys-Gly, Lys-Ala, Lys-Ser, or Lys-Gly), tripeptides (Leu-Ala-Pro, Lys-Pro-Ala, or Gly-Pro-Ala), or tetrapeptides (Lys-Trp-Ala-Pro or Lys-Pro-Ala-Ala) as the substrates. The previously described thin-layer chromatography on Silica Gel 60 F254 [22] were used to determine the activities of recombinant ApXPD towards dipeptides, tripeptides or tetrapeptides that don't contain C-terminus prolines. All of the determinations were repeated three times.

Kinetic parameters of enzymatic activity for various substrates and substrate concentrations were studied in the presence of 1 mM Co^{2+} by non-linear regression, using software Origin 2021. The Michaelis constant (K_m) and maximum velocity (V_{max}) were determined by directly fitting the Michaelis-Menten kinetic equation, $V= V_{max}S/(K_m+S)$ with the experimental data. Here V and S denote the reaction velocity and substrate concentration, respectively.

Preprints (www.preprints.org) | NOT PEER-REVIEWED | Posted: 20 October 2023 doi:10.20944/preprints202310.1370.v1

3. Results

3.1. Molecular Cloning and Sequence Analysis of the xpd Gene from A. phoenicis ATCC 14332

DNA sequencing showed that the *xpd* gene from *A. phoenicis* ATCC 14332 consisted of 1467 bp and encoded a 488-amino acid polypeptide, with the predicted molecular weight and theoretical pI of 54.9 kDa and 5.09, respectively. The DNA sequence of *xpd* gene from *A. phoenicis* ATCC 14332 matched well with that of *A. phoenicis* ATCC 13157 *xpd* gene (GenBank accession No. KZ851879.1) except for 24 nucleotide differences (data not shown). Five amino acids (Asn96, Phe125, Met360, Ala362 and Lys402) in the deduced amino acid sequence of *xpd* gene from *A. phoenicis* ATCC 14332 (Figure S1) were different from those in the amino acid sequence of *A. phoenicis* ATCC 13157 *xpd* gene, which were Asp96, Tyr125, Ile360, Thr362 and Glu402, respectively. As analyzed by SignalP 5.0 server, this enzyme didn't contain a secretory signal peptide.

3.2. Reclassification of XPDs Based on Phylogenetic Analysis and MEROPS Database

Based on the amino acid sequences of 16 available XPDs that have been molecularly and biochemically characterized, a phylogenetic tree was constructed by MEGA X. Based on the MEROPS database (version 12.5) [1], these XPDs can be grouped into three subfamilies according to their similarities to EcPEPQ (M24.003), HsPEPDI (M24.007), and PfPEPQ (M24.008), respectively, with one unassigned subfamily containing XPD from *A. phoenicis* ATCC 14332 (Figure 1). Subfamily M24.003 contains only bacterial XPDs, and M24.007 prolidases are found in eukaryotes (filamentous fungi and human), while those from subfamilies M24.008 are hyperthermophile prolidases from archaea. In the unassigned subfamily, ApXPD is the only fungal Xaa-Pro dipeptidase ever reported, whereas all other enzymes are bacterial prolidases. It has also been observed that XPDs from subfamilies M24.003, M24.007 and M24.008 exhibit hydrolytic activities toward both Xaa-Pro dipeptides and organophosphate compounds, while members of the unknown subfamily hydrolyze only Xaa-Pro dipeptides (Table S1).

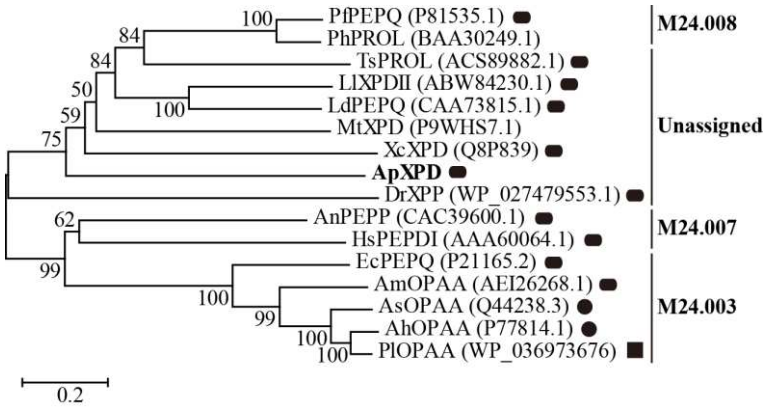

Figure 1. Evolutionary tree describing the phylogenic relationships among XPD from *A. phoenicis* ATCC 14332 (ApXPD) and all the currently characterized prolidases from various organisms. Filled circles, rounded rectangles and filled squares represent monomers, dimmers and tetramers, respectively. PfPEPQ, PhPROL, TsPROL, LlXPDII, LdPEPQ, MtXPD, XcXPD, DrXPP, AnPEPP, HsPEPDI, EcPEPQ, AmOPAA, AsOPAA, AhOPAA and PlOPAAPlOPAA are prolidases from *Pyrococcus furiosus* DSM 3638, *P. horikoshii* OT3, *Thermococcus sibiricus* MM 739, *Lactococcus lactis* NRRL B-1821, *L. delbrueckii* subsp. *bulgaricus* CNRZ 397, *Mycobacterium tuberculosis* H37Rv, *X. campestris* pv. *campestris* ATCC 33913, *Deinococcus radiodurans* R1, *A. nidulans* WG312, *Human sapiens*, *E. coli* BL21 (DE3), *Alteromonas macleodii* NCIMN1963, *Alteromonas* sp. JD6.5, *A. haloplanktis* ATCC 23851 and *Pseudoalteromonas lipolytica* SCSIO04301, respectively. GenBank accession numbers of these polidases are given in parenthesis.

Preprints (www.preprints.org) | NOT PEER-REVIEWED | Posted: 20 October 2023 doi:10.20944/preprints202310.1370.v1

As predicted by SignalP 5.0, all of these XPDs were intracellular enzymes. Variable identity percentages were found among these sequences of 16.80-89.55%, with an average of 28.40%. Among them, ApXPD shares the highest similarity (29.30%) with XcXPD but not with AnPEPP from the more related fungal species (Figure 2), while the lowest similarity (19.01%) is observed between ApXPD and DrXPP. Despite of this divergence, all the sequences could be aligned with the good conservation of the catalytic triads (His-His-His) and metal-binding residues (Asp-Asp-His-Glu-Glu) (Figure 2). Multiple sequence alignment also showed that these subfamily M24B metallopeptidases contained the conserved motifs HXXGHXXGXXXH and GXRXE (X represents any amino acid, Figure 2), where the N- and C-terminal histidines in the former motif are the nucleophiles, while the middle histidine acts as the proton receptor in the catalysis and participates in metal ion binding [23,24].

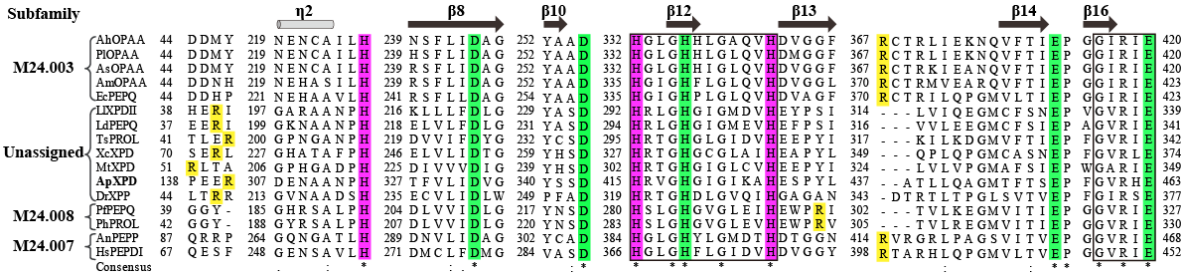

Figure 2. Multiple sequence alignment of ApXPD with all the characterized XPDs from various organisms. Prolidases from subfamilies M24.003, M24.007 and M24.008 are indicated, while other enzymes are from the unassigned subfamily. (*), the conserved amino acids; (:), the conservative replacement; (.), semiconservative replacement. Xaa-Pro dipeptidase from *A. phoenicis* ATCC 14332 is in bold. The secondary structural elements of XcXPD are shown above the sequence. The strictly conserved motifs HXXGHXXGXXXH and GXRXE (X represents any amino acid) are boxed. The putative catalytic triads, metal ion binding residues and the specific arginine residues involved in dipeptide selection are colored in purple, green and yellow, respectively.

3.3. Three-dimensional Structure Analysis of ApXPD

Using the crystal structure of XcXPD (PDB code: 5fcf) [4] as a template, the three-dimensional structure of XPD from *A. phoenicis* ATCC 14332 was built by homology modeling. As a member of 'pita-bread' family of metallopeptidases, ApXPD consists of two major domains, a small N-domain (Figure 3, creatinase/prolidase-N domain, residues 90 to 249) and a large C-terminal catalytic domain (peptidase-M24 domain, residues 250-488) [4,25,26]. N-domain contains a six-stranded mixed β-sheet flanked by six α-helices, while C-domain is formed by the pita-bread fold and has a mixed eight-stranded β-sheet with six α-helices on the outer surface. In addition, ApXPD also possesses an N-terminal tail (residues 81 to 89), which may make both polar and hydrophobic interactions with the C-domain as observed in XcXPD [4]. The putative catalytic triads of ApXPD (H314, H415 and H426) are located in an oval depression created by the pita bread fold at the centre of C-domain (Figure 3). Its putative metal-binding residues are Asp332, Asp343, His419, Glu449 and Glu463, while the specific arginine residue that mainly determines the length of ligand is supposed to be Arg141.

Preprints (www.preprints.org) | NOT PEER-REVIEWED | Posted: 20 October 2023 doi:10.20944/preprints202310.1370.v1

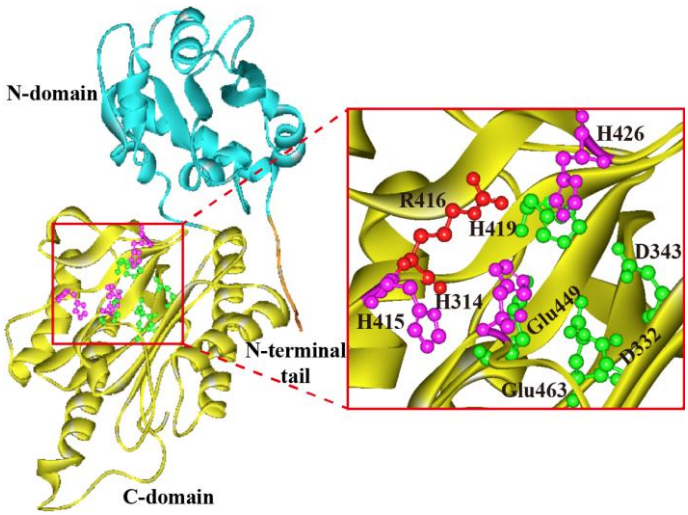

Figure 3. Molded 3D structure of XPD from *A. phoenicis* ATCC 14332. Regions of N-terminal tail, N-domain, and C-domain are shown in orange, light blue and yellow colors, respectively. Putative catalytic triads (His314, His415 and H426), metal ion binding residues (Asp332, Asp343, His419, Glu449 and Glu463) and the specific arginine residue (Arg416) that determines the length of ligand are represented by purple, green, and red scaled ball and sticks, respectively.

3.4. Expression and Purification of Recombinant ApXPD

The recombinant plasmid pPIC9K-xpd was linearized with *Sac*I and electroporated into *P. pastoris* GS115, generating the recombinant GS115 (pPIC9K-apxpd). After five days of shake flask fermentation, the activity of this recombinant towards Lys-Pro was determined to be 35.5±4.1 U/mL, whereas no XPD activity could be detected in the strain GS115-9K (*P. pastoris* GS115 integrated with pPIC9K). This enzyme was then partially purified to homogeneity by ammonium sulfate precipitation, dialysis and ultrafiltration (Figure 4), with a yield of the purified ApXPD of 28.7 mg/L culture. SDS-PAGE analysis indicated that the purified ApXPD migrated as a single band corresponding to a molecular mass of approximately 55.0 kDa (Figure 4), while it exhibited a single protein peak at a molecular weight corresponding ~110 kDa on gel-filtration chromatography (data not shown), suggesting that ApXPD exists as a dimer under the given conditions. Besides, the specific activity of the purified ApXPD towards Lys-Pro was 51.2 U/mg.

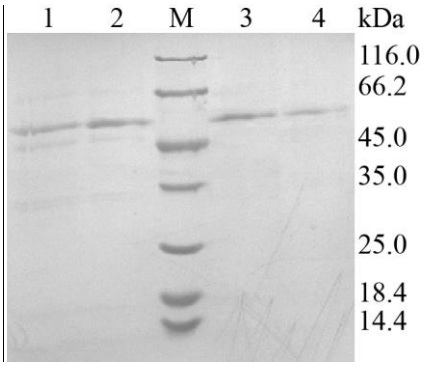

Figure 4. SDS-PAGE analysis on the expression and purification of ApXPD. Lanes 1 and 2, cell-free supernatants of the recombinant strain; lanes 3 and 4, the purified ApXPD; M, molecular mass markers; the bands at approximately 55.0 kDa represent target proteins.

3.5. Effects of Temperature and pH on the Activity and Stability of Recombinant ApXPD

Effects of temperature and pH on the activity and stability of ApXPD were examined. As shown in Figure 5, this enzyme was active at temperatures ranging from 20 to 70°C. It maintained over 80% of the maximum activity at temperatures of 50-60°C, and the highest activity was observed at 55°C.

Preprints (www.preprints.org) | NOT PEER-REVIEWED | Posted: 20 October 2023 doi:10.20944/preprints202310.1370.v1

Recombinant ApXPD was stable at 20 and 30°C because it retained more than 80% of the activity after treatment at these temperatures for 1 h. After 1-h incubation at 40, 50 and 60°C, its activity was reduced to 71.5%, 55.7% and 39.0% of the original level, respectively, while 31.1% activity remained after incubation at 70°C for 1 h.

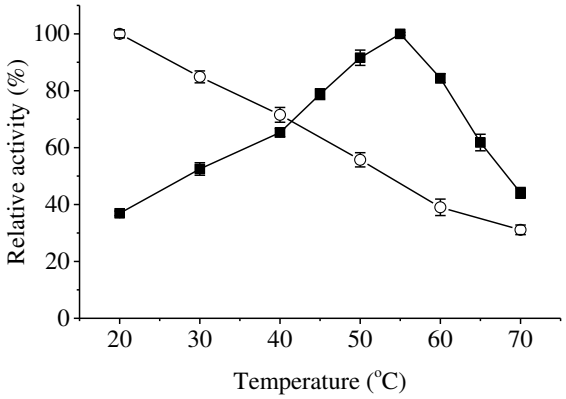

Figure 5. Effects of temperature on the activity (closed squares) and stability (open circles) of ApXPD. The relative activity is calculated with the highest activity regarded as 100%.

The optimum pH of ApXPD was determined at various pHs using three different buffer solutions at 55°C. As shown in Figure 6A, recombinant ApXPD was optimally active at pH 9.0, and it retained more than 80% of the maximal activity between pH 8.5-10.5. This enzyme was stable over a narrow pH range of 8.5-10.0, with over 80% residual activities after 1-h incubation at 55°C (Figure 6B).

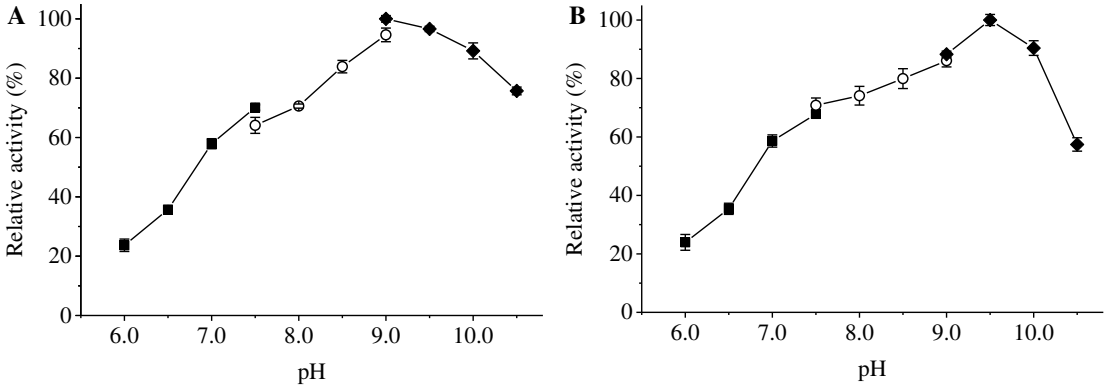

Figure 6. Effects of pH on the activity (**A**) and stability (**B**) of ApXPD. The relative activity is calculated with the maximum activity set as 100%. Filled circles, open squares, and filled diamonds represent 20 mM sodium citrate buffer (pH 6.0-7.5), 20 mM Tris-HCl buffer (pH 7.5-9.0) and 20 mM glycine-NaOH buffer (pH 9.0-10.5), respectively.

3.6. Effects of Various Chemicals on the Activity of Recombinant ApXPD

Effects of various metal ions on the activity of recombinant ApXPD were shown in Table 1. Among the metal ions tested, 0.1 mM and 1 mM Ca^{2+}, Zn^{2+}, Cu^{2+} and Fe^{3+} strongly inhibited the activity of ApXPD, and their inhibitory effects increased with the increasing concentrations. EDTA also exerted inhibitory effects on the activity of ApXPD, indicating that this enzyme is metal ion-dependent [4]. On the contrary, the activity of this enzyme was significantly enhanced by 0.1 mM and 1 mM Mn^{2+}, Co^{2+} and Sn^{2+}. Besides, its activity was increased by two fold by 1 mM Co^{2+} (Table 1), which suggests that cobalt is possibly the cofactor of ApXPD.

Preprints (www.preprints.org) | NOT PEER-REVIEWED | Posted: 20 October 2023 doi:10.20944/preprints202310.1370.v1

Table 1. Effects of metal ions and chemicals on the activity of recombinant ApXPD.

Metal ions	Concentration (mM)	Relative Activity (%)
None	0	100
$CaCl_2$	0.1	82.1 ± 0.4
	1	53.8 ± 0.9
$ZnCl_2$	0.1	102.6 ± 0.9
	1	89.7 ± 3.1
$MnCl_2$	0.1	114.7 ± 1.6
	1	104.5 ± 1.4
$CuCl_2$	0.1	64.7 ± 0.7
	1	25.6 ± 0.3
$CoCl_2$	0.1	136.5 ± 1.5
	1	300.6 ± 2.6
$SnCl_2$	0.1	203.2 ± 2.2
	1	166.0 ± 1.9
$FeCl_3$	0.1	96.8 ± 0.6
	1	87.8 ± 1.6
EDTA	0.1	92.1 ± 0.3
	1	76.5 ± 1.1

3.7. Substrate Specificity of Recombinant ApXPD

Among the substrates tested, recombinant ApXPD hydrolyzed dipeptides Lys-Pro , Gly-Pro and Ala-Pro, but it didn't cleave other dipeptides, tripeptides and tetrapeptides tested (Table 2). Besides, this enzyme also didn't exhibit hydrolytic activities towards amino acid *p*-nitroanilides (Glu-, Arg-, Ile-, Met, Asp-, Glu-, His-, Phe-, Pro-, Trp-, Tyr- and Val-*p*NA), and *N*-carbobenzoxy-dipeptides, including CBZ-Ala-Arg, CBZ-Pro-Gly, CBZ-Ala-Lys, CBZ-Gly-Ala, CBZ-Ala-Glu, and CBZ-Phe-Leu (data not shown). All these results indicated that ApXPD was exclusively a Xaa-Pro dipeptidase but not an aminopeptidase or carboxypeptidase.

Table 2. Substrate specificity of recombinant ApXPD.

Substrate	Relative Activity (%)
Lys-Pro†	100 ± 2.1
Gly-Pro†	86.3 ± 1.7
Ala-Pro†	32.7 ± 1.3
Pro-Pro†	ND
Cys-Gly *	—
Lys-Ala *	—
Lys-Ser *	—
Lys-Gly *	—
Leu-Ala-Pro†	ND
Lys-Pro-Ala *	—
Gly-Pro-Ala *	—
Lys-Trp-Ala-Pro†	ND
Lys-Pro-Ala-Ala *	—

† Prolidase activity was measured by assaying the release of proline using the modified ninhydrin method; ND, not detected. * Thin-layer chromatography on Silica Gel 60 F254 was used to look for a release of the N-terminal amino acid. —, No release of amino acid observed.

3.8. Enzyme Kinetics

Kinetic parameters were determined for recombinant ApXPD using Lys-Pro and Gly-Pro as substrates (Table 3). As compared with Gly-Pro, recombinant ApXPD showed high affinity for Lys-

Preprints (www.preprints.org) | NOT PEER-REVIEWED | Posted: 20 October 2023 doi:10.20944/preprints202310.1370.v1

Pro as indicated by the low K_m value. Additionally, high values of V_{max}, k_{cat} and k_{cat}/K_m were observed for Lys-Pro, suggesting its high reaction velocity and catalytic efficiency against this substrate.

Table 3. Kinetic parameters of recombinant ApXPD.

Substrate	V_{max} (μmol min^{-1} mg^{-1})	K_m (mM)	k_{cat} (s^{-1})	k_{cat}/K_m (mM^{-1} s^{-1})
Lys-Pro	85.7	1.0	123.5	123.5
Gly-Pro	82.8	1.2	105.9	88.3

4. Discussion

To date, more than 20 microbial Xaa-Pro dipeptidases have been molecularly and/or biochemically characterized. Among them, the prolidase from *Aureohacterium esteraromaticum* [27] is possibly not a prolidase since it lacks the corresponding active site and metal-binding residues of prolidases as shown by multiple sequence alignment (data not shown). Previously, prokaryotic prolidases have been classified into two subfamilies (XPDxc-type and XPD48-type) according to their molecular weights and sequence relatedness [4,9,25]. However, this classification system may cause confusions as observed for prolyl aminopeptidases [28]. In the present study, based on sequence relatedness and structural similarity, the 16 Xaa-Pro dipeptidases that have been molecularly and biochemically characterized were reclassified into 4 subfamilies by the MEROPS classification system: M24.003, M24.007, M24.008 and one unassigned subfamily (Figure 1). Prolidases from the unassigned subfamily and subfamilies M24.007 and M24.008 are mainly dimers, whereas subfamily M24.003 contains monomers, dimers and even a tetramer (Figure 1 and Table S1). Multiple sequence alignment demonstrated that four regions containing at least ten residues were present in prolidases from subfamilies M24.003 and M24.007 but absent in members from M24.008 and the unassigned subfamily (Figure S1). In these regions, three residues (EcPEPQ numbering: residues Pro363, Leu369 and Arg370) are strictly conserved. Besides, an N-terminal loop extension has been found in prolidases from the M24.007 (AnPEPP and HsPEPDI) and unknown (XcXPD, MtXPD and ApXPD) subfamilies (Figure S1). Xaa-Pro dipeptidases from subfamily M24.003 only exist in bacteria, and subfamily M24.007 contains prolidases from eukaryotes (fungi and human), while enzymes from subfamilies M24.008 proteins are prolidases from hyperthermophilic archaea. In the unassigned subfamily, all prolidases are from bacteria except ApXPD, which is the only reported fungal Xaa-Pro dipeptidase containing an additional region (PAPARLREKL, residues 361-370; Figure S1). Interestingly, ApXPD also shares the highest sequence similarity with XcXPD [4,29], but not with the prolidase from the more related fungal species *A. nidulans* (AnPEPP, Figure 2). Therefore, XPD from *A. phoenicis* ATCC 14332 represents a novel Xaa-Pro dipeptidase subfamily.

Xaa-Pro dipeptidases differ greatly in their optimal temperatures, optimal pHs, metal requirements and substrate specificities. The optimum temperature of ApXPD was 55°C (Figure 5), which was the same as or higher than those of prolidases from mesophilic sources [2], but much lower than the optimal temperatures (100°C) of prolidases derived from hyperthermophilic archaea *Pyrococcus* ssp. [21,30]. Most XPDs are stable at low temperatures (20-50°C), as is the case of XPD from *A. phoenicis* ATCC 14332. Unlike most prolidases, which are most active under acidic or neutral pHs (pH 6.0-8.5), ApXPD acts optimally under more alkaline pH (pH 9.0) and is stable over a narrow pH range of 8.5-10.0 (Figure 6).

XPDs require one or two divalent cations for enzyme activity, typically Mn^{2+}, Co^{2+} or Zn^{2+} [31,32]. *In vitro* studies have shown that most prolidases ever reported utilize Mn^{2+} ion as cofactors (Table S1) [4,24,33-36], whereas PfPEPQ, PhPROL and ScXPD require Co^{2+} in their active sites under aerobic assay conditions [21,30,37], as is the case of XPD from *A. phoenicis* ATCC 14332 (Table 1). Besides, the enzymatic activities of LdPEPQ, LlXPDII, and TsPROL are dependent on Zn^{2+} [22,38,39]. In contrast, the activities of AsOPAA, AuOPAA, LcXPD, PfpepQ, PhPROL and XmXPD were strongly or even completely inactivated by high concentrations of Zn^{2+} (Table S1), which is due to the fact that Zn binding decreases the volume of active site pocket for accumulating the substrates [26]. Since the *in vivo* concentrations of Mn^{2+} and Co^{2+} are much lower than that of Zn^{2+}, the metal ion requirements for XPDs *in vivo* are quite different and a preference for Zn^{2+} might be advantageous [40]. Moreover,

 doi:10.20944/preprints202310.1370.v1

PfPEPQ and PhPROL require Fe^{2+} rather than Co^{2+} for maximal activity under anaerobic conditions, suggesting that their metal preferences *in vivo* may be changed [30,31].

XPDs are highly specific in the type of substrate that they hydrolyze, and they usually prefer dipeptides to tripeptides and tetrapeptides. Prolidases from subfamilies M24.003, M24.007 and M24.008 hydrolyze both Xaa-Pro dipeptides and OP compounds, whereas those from the unassigned subfamily only cleave Xaa-Pro dipeptides (Table S1). There are also some differences in dipeptide substrate specificities among the prolidases that have been biochemically characterized. Their main activity is Xaa-Pro dipeptides hydrolysis, although several prolidases can cleave dipeptides with proline at the N-terminus or dipeptides that do not contain a proline residue [36,39,41]. Most prolidases show broad substrate specificities and prefer Xaa-Pro dipeptides containing N-terminal hydrophobic amino acids, whereas PfPEPQ [21], PhPROL [30] and EcPEPQ [33] show affinity for negatively charged and/or hydrophilic amino acids at the N-terminus. The recombinant ApXPD characterized in this study, however, shows preference for positively charged Lys-Pro (Tables 2 and 3). Besides, most prolidases don't hydrolyze Pro-Pro and Gly-Pro except MtXPD [4], XcXPD [4], AnPEPP [15], PlOPAA [35], DrXPP [39], and HsPEPDI [42].

Typically, the substrate length of prolidases is restricted to dipeptides by the guanidinium side chain of an arginine residue that binds to the free carboxylate of dipeptides and prevents the binding of longer peptides [4,9,25,43]. Besides, the specific arginine residue can also increase the affinities of XPDs for substrates by introducing allosteric behavior and substrate inhibition [4,23,44]. Prolidases from these four subfamilies vary greatly in their specific arginine residues. As shown by multiple sequence alignment in Figure 2, the specific arginine residues of subfamily M24.003 prolidases are counterparts of those in XPDs from subfamily M24.007, such as Arg370 in AmOPAA [9], Arg370 in EcPEPQ [43] as well as Arg398 in HsPEPDI [45], while the arginine residues in PfPEPQ and PhPROL from subfamily M24.008 are Arg295 and Arg298 [38], respectively, which do not correspond to those in subfamilies M24.003 and M24.007 XPDs (Figure 2). Unlike XPDs in other three subfamilies, however, prolidases from the unassigned subfamily use a novel arginine dependent mechanism for dipeptide selectivity. According to the results of structural, mutational and/or molecular dynamics simulation analyses, the corresponding arginine residues employed by XcXPD [4], DrXPP [39] and LlXPDII [44] have been found to be Arg72, Arg46 and Arg40, respectively, while the equivalent residue in ApXPD is Arg141 (Figure 2). Further understanding and study of the precise mechanism of prolidases from the unassigned subfamily used for dipeptide selectivity is highly warranted. Aside from structural differences in the substrate binding pocket, the variability of prolidase substrate specificity also depends on the catalytic metal cation [4,23,38]. For example, in the presence of Mn^{2+}, LlXPDII shows low activity towards Pro-Pro, whereas it can't hydrolyze this dipeptide in the presence of Zn^{2+}. Furthermore, its substrate preference changes from Leu-Pro to Arg-Pro in the presence of Mn^{2+} [38].

5. Conclusions

In summary, a Xaa-Pro dipeptidase from *A. phoenicis* ATCC 14332 was molecularly and biochemically characterized. Phylogenetic analysis showed that this enzyme was the only fungal XPD in the unassigned subfamily, and it shared the highest sequence similarity with XcXPD but not with AnPEPP from the more related species. Multiple sequence alignment and 3D structure modeling revealed that it contained an additional region of PAPARLREKL and an N-terminal tail (residues 81-89), and utilized a different arginine residue for dipeptide selectivity. Taken together with of its distinct biochemical properties, including high stability under alkaline conditions, specific metal requirement and substrate specificity, our results indicate that recombinant ApXPD represents a novel prolidase subfamily. Knowledge gained here not only brings some new knowledge in the area of fungal XPDs but also provides a firm foundation for future research on the industrial application and *in vivo* physiological roles of this fungal Xaa-Pro dipeptidase.

Supplementary Materials: The following supporting information can be downloaded at the website of this paper posted on Preprints.org, Figure S1: Multiple sequence alignment of ApXPD with all the characterized XPDs from various organisms; Table S1: Xaa-Pro dipeptidases that have been characterized by molecular and/or biochemical techniques.

Author Contributions: Conceptualization, Z.D. and L.Y.; methodology, Z.D., S.Y. and K.Z.; software, S.Y. and K.Z.; validation, Z.D. and Y.K.; formal analysis, Z.D. and C.T.; investigation, S.Y. and C.T.; writing—original draft preparation, Z.D. and S.Y.; writing—review and editing, Y.K. and L.Y.; visualization, Z.D. and S.Y.; supervision, Z.D. and L.Y.; funding acquisition, Z.D. All authors have read and agreed to the published version of the manuscript.

Funding: This research was funded by the Specialized Research Fund for the Doctoral Program of Nanyang Normal University (grant No. 2020ZX004), Training Program for National Natural Science Foundation of China by Nanyang Normal University (grant No. 2023Y005) and the Henan Province Natural Science Foundation (grant No. 222300420251).

Data Availability Statement: The data presented supporting the findings of this study are available from the corresponding author upon request.

Conflicts of Interest: The authors declare no conflict of interest.

References

1. Rawlings, N.D.; Alan, J.; Thomas, P.D.; Huang, X.D.; Bateman, A.; Finn, R.D. The MEROPS database of proteolytic enzymes, their substrates and inhibitors in 2017 and a comparison with peptidases in the PANTHER database. *Nucleic Acids Res.* **2018**, *46*, D624-D632.
2. Kitchener, R.; Grunden, A. Prolidase function in proline metabolism and its medical and biotechnological applications. *J. Appl. Microbiol.* **2012**, *113*, 233-247.
3. Namiduru, E.S. Prolidase. *Bratisl. Lek. Listy.* **2016**, *117*, 480-485.
4. Are, V.N.; Kumar, A.; Kumar, S.; Goyal, V.D.; Ghosh, B.; Bhatnagar, D.; Jamdar, S.N.; Makde, R.D. Crystal structure and biochemical investigations reveal novel mode of substrate selectivity and illuminate substrate inhibition and allostericity in a subfamily of Xaa-Pro dipeptidases. *BBA-Proteins Proteom.* **2017**, *1865*, 153-164.
5. Wilk, P.; Wator, E.; Weiss, M.S. Prolidase - A protein with many faces. *Biochimie* **2021**, *183*, 3-12.
6. Misiura, M.; Miltyk, W. Current understanding of the emerging role of prolidase in cellular metabolism. *Int. J. Mol. Sci.* **2020**, *21*, 5906.
7. Eni-Aganga, I.; Lanaghan, Z.M.; Balasubramaniam, M.; Dash, C.; Pandhare, J. PROLIDASE: A review from discovery to its role in health and disease. *Front. Mol. Biosci.* **2021**, *8*, 723003.
8. Theriot, C.M.; Tove, S.R.; Grunden, A.M. Chapter 3 Biotechnological applications of recombinant microbial prolidases. In *Adv. Appl. Microbiol.*; Academic Press: 2009; Volume 68, pp. 99-132.
9. Stepankova, A.; Duskova, J.; Skalova, T.; Hasek, J.; Koval, T.; Ostergaard, L.H.; Dohnalek, J. Organophosphorus acid anhydrolase from *Alteromonas macleodii*: structural study and functional relationship to prolidases. *Acta Crystallogr. Sect. F Struct. Biol. Cryst. Commun.* **2013**, *69*, 346-354.
10. Manco, G.; Porzio, E.; Suzumoto, Y. Enzymatic detoxification: a sustainable means of degrading toxic organophosphate pesticides and chemical warfare nerve agents. *J. Chem. Technol. Biot.* **2018**, *93*, 2064-2082.
11. Wang, T.-F.; Lo, H.-F.; Chi, M.-C.; Lai, K.-L.; Lin, M.-G.; Lin, L.-L. Affinity immobilization of a bacterial prolidase onto metal-ion-chelated magnetic nanoparticles for the hydrolysis of organophosphorus compounds. *Int. J. Mol. Sci.* **2019**, *20*, 3625.
12. Yang, J.; Xiao, Y.-Z.; Li, R.; Liu, Y.; Long, L.-J. Repurposing a bacterial prolidase for organophosphorus hydrolysis: Reshaped catalytic cavity switches substrate selectivity. *Biotechnol. Bioeng.* **2020**, *117*, 2694-2702.
13. Yang, J.; Xiao, Y.; Liu, Y.; Li, R.; Long, L. Structure-based redesign of the bacterial prolidase active-site pocket for efficient enhancement of methyl-parathion hydrolysis. *Catal. Sci. Technol.* **2021**, *11*, 5086-5093.
14. Spodenkiewicz, M.; Spodenkiewicz, M.; Cleary, M.; Massier, M.; Fitsialos, G.; Cottin, V.; Jouret, G.; Poirsier, C.; Doco-Fenzy, M.; Lèbre, A.S. Clinical genetics of prolidase deficiency: An updated review. *Biology (Basel)* **2020**, *9*, 108.
15. Jalving, R.; Bron, P.; Kester, H.C.; Visser, J.; Schaap, P.J. Cloning of a prolidase gene from *Aspergillus nidulans* and characterisation of its product. *Mol. Genet. Genomics* **2002**, *267*, 218-222.
16. Ameen, F.; AlNadhari, S.; Yassin, M.A.; Al-Sabri, A.; Almansob, A.; Alqahtani, N.; Stephenson, S.L. Desert soil fungi isolated from Saudi Arabia: cultivable fungal community and biochemical production. *Saudi J. Biol. Sci.* **2022**, *29*, 2409-2420.
17. Li, Q.; Loman, A.A.; Coffman, A.M.; Ju, L. Soybean hull induced production of carbohydrases and protease among *Aspergillus* and their effectiveness in soy flour carbohydrate and protein separation. *J. Biotechnol.* **2017**, *248*, 35-42.

18. N., K.C.; J., D.; Z., M.; L., D.; T., H.; P., W.J.; Ph, T. Optimization of extracellular catalase production from *Aspergillus phoenicis* K30 by Plackett-Burman design and linear regression using date flour as single carbon source and purification of the enzyme. *Afr. J. Biotechnol.* **2013**, *12*, 2646-2653.
19. Iwasa, H.; Ozawa, K.; Sasaki, N.; Kinoshita, N.; Yokoyama, K.; Hiratsuka, A. Fungal FAD-dependent glucose dehydrogenases concerning high activity, affinity, and thermostability for maltose-insensitive blood glucose sensor. *Biochem. Eng. J.* **2018**, *140*, 115-122.
20. Kumar, S.; Stecher, G.; Li, M.; Knyaz, C.; Tamura, K. MEGA X: Molecular evolutionary genetics analysis across computing platforms. *Mol. Biol. Evol.* **2018**, *35*, 1547-1549.
21. Ghosh, M., .; Grunden, A.M.; Dunn, D.M.; Weiss, R., .; Adams, M.W. Characterization of native and recombinant forms of an unusual cobalt-dependent proline dipeptidase (prolidase) from the hyperthermophilic archaeon *Pyrococcus furiosus*. *J. Bacteriol.* **1998**, *180*, 4781-4789.
22. Morel, F.; Frot-Coutaz, J.; Aubel, D.; Portalier, R.; Atlan, D. Characterization of a prolidase from *Lactobacillus delbrueckii* subsp. *bulgaricus* CNRZ 397 with an unusual regulation of biosynthesis. *Microbiology* **1999**, *145 (Pt 2)*, 437.
23. Kgosisejo, O.; Chen, J.A.; Grochulski, P.; Tanaka, T. Crystallographic structure of recombinant *Lactococcus lactis* prolidase to support proposed structure-function relationships. *BBA-Proteins Proteom.* **2017**, *1865*, 473-480.
24. Besio, R.; Alleva, S.; Forlino, A.; Lupi, A.; Meneghini, C.; Minicozzi, V.; Profumo, A.; Stellato, F.; Tenni, R.; Morante, S. Identifying the structure of the active sites of human recombinant prolidase. *Eur. Biophys. J.* **2010**, *39*, 935-945.
25. Maher, M.J.; Ghosh, M.; Grunden, A.M.; Menon, A.L.; Adams, M.W.W.; Adams, M.W.W.; Freeman, H.C.; Guss, J.M. Structure of the prolidase from *Pyrococcus furiosus*. *Biochemistry* **2004**, *43*, 2771-2783.
26. Jeyakanthan, J.; Takada, K.; Sawano, M.; Ogasahara, K.; Mizutani, H.; Kunishima, N.; Yokoyama, S.; Yutani, K. Crystal structural and functional analysis of the putative dipeptidase from *Pyrococcus horikoshii* OT3. *J. Biophys.* **2009**, *2009*, 434038.
27. Kabashima, T.; Fujii, M.; Hamasaki, Y.; Ito, K.; Yoshimoto, T. Cloning of a novel prolidase gene from *Aureobacterium esteraromaticum*. *BBA-Mol. Cell Res.* **1999**, *1429*, 516-520.
28. Mahon, C.S.; O'Donoghue, A.J.; Goetz, D.H.; Murray, P.G.; Craik, C.S.; Tuohy, M.G. Characterization of a multimeric, eukaryotic prolyl aminopeptidase: an inducible and highly specific intracellular peptidase from the non-pathogenic fungus *Talaromyces emersonii*. *Microbiology* **2009**, *155*, 3673-3682.
29. Kumar, A.; Are, V.N.; Ghosh, B.; Agrawal, U.; Jamdar, S.N.; Makde, R.D.; Sharma, S.M. Crystallization and preliminary X-ray diffraction analysis of Xaa-Pro dipeptidase from *Xanthomonas campestris*. *Acta Crystallogr. F Struct. Biol. Commun.* **2014**, *70*, 1268-1271.
30. Theriot, C.M.; Tove, S.R.; Grunden, A.M. Characterization of two proline dipeptidases (prolidases) from the hyperthermophilic archaeon *Pyrococcus horikoshii*. *Appl. Microbiol. Biotechnol.* **2010**, *86*, 177-188.
31. Du, X.L.; Tove, S.; Kast-Hutcheson, K.; Grunden, A.M. Characterization of the dinuclear metal center of *Pyrococcus furiosus* prolidase by analysis of targeted mutants. *FEBS Lett.* **2005**, *579*, 6140-6146.
32. Besio, R.; Baratto, M.C.; Gioia, R.; Monzani, E.; Nicolis, S.; Cucca, L.; Profumo, A.; Casella, L.; Basosi, R.; Tenni, R.; et al. A Mn(II)–Mn(II) center in human prolidase. *BBA - Proteins and Proteom.* **2013**, *1834*, 197-204.
33. Park, M.S.; Hill, C.M.; Li, Y.; Hardy, R.K.; Khanna, H.; Khang, Y.H.; Raushel, F.M. Catalytic properties of the PepQ prolidase from *Escherichia coli*. *Arch. Biochem. Biophys.* **2004**, *429*, 224-230.
34. Vyas, N.K.; Nickitenko, A.; Rastogi, V.K.; Shah, S.S.; Quiocho, F.A. Structural insights into the dual activities of the nerve agent degrading organophosphate anhydrolase/prolidase. *Biochemistry* **2010**, *49*, 547-559.
35. Xiao, Y.Z.; Yang, J.; Tian, X.P.; Wang, X.X.; Li, J.; Zhang, S.; Long, L.J. Biochemical basis for hydrolysis of organophosphorus by a marine bacterial prolidase. *Process Biochem.* **2017**, *52*, 141-148.
36. Fernandez-Espla, M.D.; Martin-Hernandez, M.C.; Fox, P.F. Purification and characterization of a prolidase from *Lactobacillus casei* subsp. *casei* IFPL 731. *Appl. Environ. Microbiol.* **1997**, *63*, 314-316.
37. Kaminogawa, S.; Azuma, N.; Hwang, I.K.; Suzuki, Y.; Yamauchi, K. Isolation and characterization of a prolidase from *Streptococcus cremoris* H61. *J. Agr. Chem. Soc. JPN.* **1984**, *48*, 3035-3040.
38. Yang, S.I.; Tanaka, T. Characterization of recombinant prolidase from *Lactococcus lactis*- changes in substrate specificity by metal cations, and allosteric behavior of the peptidase. *FEBS J.* **2008**, *275*, 271-280.
39. Are, V.N.; Jamdar, S.N.; Ghosh, B.; Goyal, V.D.; Kumar, A.; Neema, S.; Gadre, R.; Makde, R.D. Crystal structure of a novel prolidase from *Deinococcus radiodurans* identifies new subfamily of bacterial prolidases. *Proteins* **2017**, *85*, 2239-2251.
40. Willingham, K.; Maher, M.J.; Grunden, A.M.; Ghosh, M.; Adams, M.W.W.; Freeman, H.C.; Guss, J.M. Crystallization and characterization of the prolidase from *Pyrococcus furiosus*. *Acta Crystallogr. D* **2001**, *57*, 428-430.
41. Cheng, T.; Liu, L.; Wang, B.; Wu, J.; DeFrank, J.J.; Anderson, D.M.; Rastogi, V.K.; Hamilton, A.B. Nucleotide sequence of a gene encoding an organophosphorus nerve agent degrading enzyme from *Alteromonas haloplanktis*. *J. Ind. Microbiol. Biotechnol.* **1997**, *18*, 49-55.

42. Lupi, A.; Della Torre, S.; Campari, E.; Tenni, R.; Cetta, G.; Rossi, A.; Forlino, A. Human recombinant prolidase from eukaryotic and prokaryotic sources. Expression, purification, characterization and long-term stability studies. *FEBS J.* **2006**, *273*, 5466-5478.
43. Weaver, J.; Watts, T.; Li, P.; Rye, H.S. Structural basis of substrate selectivity of *E. coli* prolidase. *PLoS One* **2014**, *9*, e111531.
44. Chen, J.A.; Tanaka, T. Charged residues on a flap-loop structure of *Lactococcus lactis* prolidase play critical roles in allosteric behavior and substrate inhibition. *BBA-Proteins Proteom.* **2011**, *1814*, 1677-1685.
45. Wilk, P.; Uehlein, M.; Kalms, J.; Dobbek, H.; Mueller, U.; Weiss, M.S. Substrate specificity and reaction mechanism of human prolidase. *FEBS J.* **2017**, *284*, 2870-2885.